Proc. Natl. Acad. Sci. USA
Vol. 90, pp. 5519–5523, June 1993
Cell Biology

A motility in the eukaryotic flagellum unrelated to flagellar beating

(*Chlamydomonas*/intracellular movement/ultrastructure)

KEITH G. KOZMINSKI, KARL A. JOHNSON, PAUL FORSCHER, AND JOEL L. ROSENBAUM*

Department of Biology, Yale University, New Haven, CT 06511-8112

Communicated by Hewson Swift, March 17, 1993

ABSTRACT **We report a motility in the flagella of the green alga *Chlamydomonas* that is unrelated to dynein-based flagellar beating. This motility, referred to as intraflagellar transport, was observed as the rapid bidirectional movement of granule-like particles along the length of the flagella. Intraflagellar transport could be experimentally separated from other, previously reported, nonbeat flagellar motilities. EM of flagella showed groups of nonvesicular, lollipop-shaped structures positioned between the outer doublet microtubules and the flagellar membrane. Movement of these complexes along the length of the flagella may be responsible for intraflagellar transport.**

Flagellar motility is commonly equated with flagellar beating. Yet over the past 40 years, three motilities unrelated to dynein-mediated flagellar beating have been observed in the eukaryotic flagellum. All three have been studied primarily in the biflagellate alga *Chlamydomonas* and have been attributed to the movement of glycoproteins in the plane of the flagellar membrane (for review, see refs. 1 and 2). These membrane-associated motilities are the gliding of cells by means of their flagella across surfaces (3, 4), the saltatory bidirectional movement of polystyrene beads attached to the surface of the flagellar membrane (5), and the mobilization of glycoproteins from positions along the length of the flagella to the flagellar tips during the mating process (ref. 6; for review, see ref. 7). Pharmacological evidence suggests that all three of these nonbeat motilities are related, sharing the same motors or regulatory mechanisms (for review, see refs. 1 and 2).

While reexamining these three motilities with video-enhanced differential interference-contrast (DIC) microscopy, we were surprised to find a fourth, previously unobserved, nonbeat motility within the flagella of *Chlamydomonas*. In prior light microscopic studies, the flagella of *Chlamydomonas* have always been observed as relatively featureless high-contrast rods. Therefore, the visualization of granule-like particles moving bidirectionally along the length of the flagella, apparently between the microtubular axoneme and flagellar membrane, was striking. In addition, improved fixation methods for EM have allowed for the routine observation, in thin section, of complexes between the flagellar membrane and the axonemal microtubules. The movement of these complexes may account for this motility, referred to as intraflagellar transport (IFT).

MATERIALS AND METHODS

Cultures. *Chlamydomonas moewusii* strains M475 (CC 957) and gf1 (CC 1371) and *Chlamydomonas reinhardtii* strains pf1 (CC 1024), pf18 (CC 1036), and pf28 (CC 1877) were obtained from the *Chlamydomonas* Genetics Center (Duke University, Durham, NC). *C. moewusii* was favored for video-enhanced DIC microscopy because their flagella are ≈50% longer than those of *C. reinhardtii*. The paralyzed flagellar dynein triple-mutant ida2 ida4 oda6 of *C. reinhardtii* was from R. Kamiya (Nagoya University). Logarithmic-phase, synchronously dividing cultures were grown in minimal medium (MI) (8) on a 12 hr:12 hr light/dark cycle with continuous aeration.

Flagellar Regeneration and Resorption. Flagellar regeneration was induced by pH-shock (9). After deflagellation, the cells were washed with fresh MI medium. Flagellar resorption was induced by placing the cells in a low-Ca^{2+}, high-Na^{+} medium (10) or also, with *C. reinhardtii*, by adding 3-isobutyl-1-methylxanthine to MI medium at a final concentration of 0.5 mM (11).

Video Microscopy. For all experiments, cultures were diluted 1:5 with double-distilled water and placed between two acid-washed no. 1 coverslips (Corning) supported with 1-mm plastic shims affixed with Vaseline. When required, polystyrene beads with a 0.3-μm diameter (Polysciences), washed four times with double-distilled water, were mixed with the cells to a final dilution of 1:500. Dilution of the culture medium enhanced the attachment of beads to the flagellar membrane. All experiments were done at room temperature using a Zeiss Axiovert microscope. The optics and method of digital data acquisition have been detailed (12), except that the light source used in this study was passed through a fiber optic scrambler to obtain full and even illumination of the condenser (1.4 N.A.) back focal plane.

For further analysis of IFT, inhibitors (Sigma) were mixed with the cell preparation to the final concentrations indicated. Aliquots were then added to the coverslip chamber. To reverse inhibition, fresh MI medium was perfused into the chamber. To reverse EGTA treatment, $CaCl_2$ was added to 1 mM in the perfusing medium.

Image Processing and Analysis. Rates of gliding, bead translocation, and IFT were made as described (13). To enhance contrast, as in Fig. 1*B*, IFT images were captured from an optical disk recording and passed through a shift/difference filter and a 5 × 5 pixel convolution filter (Adobe Photoshop, Mountain View, CA) by using a Nuvista video digitizing board (TrueVision, Indianapolis) and a Macintosh IIfx computer. To enhance motion detection, a difference-image, as shown in Fig. 1*C*, was produced by subtracting each image in the sequence from the image at the previous time point, by using a custom macro program written for IMAGE 1 (Wayne Rasband, National Institutes of Health) that allows only moving objects to be visualized.

EM. Vegetative cells were fixed in 3% glutaraldehyde/10 mM Hepes, pH 7.2 for 2 hr at 4°C, warmed briefly, and then included in a block of low-melting temperature agarose. The cells were postfixed in 1% OsO_4/0.8% K_3FeCN/4 mM phosphate buffer, pH 7.2 for 30 min at 4°C, and then *en bloc*

The publication costs of this article were defrayed in part by page charge payment. This article must therefore be hereby marked "*advertisement*" in accordance with 18 U.S.C. §1734 solely to indicate this fact.

Abbreviations: IFT, intraflagellar transport; DIC, differential interference-contrast.

*To whom reprint requests should be addressed at: 310 Kline Biology Tower, Yale University, P.O. Box 6666, New Haven, CT 06511-8112.

stained in 2% uranyl acetate for 2 hr at room temperature. This is a modification of a published procedure (14). Cells were then dehydrated through an ethanol series to propylene oxide and embedded in Embed 812 (Electron Microscopy Sciences, Fort Washington, PA). Silver/gold thin sections were cut with a diamond knife and stained with uranyl acetate and lead citrate. EM was done on a Philips EM 201; photographs were taken on Kodak EM4489 film and developed according to the manufacturer's instructions.

RESULTS

By using cells with nonbeating (paralyzed) flagella to facilitate observation with video-enhanced DIC microscopy, a previously unobserved motility was detected in the flagella of *Chlamydomonas*. This motility, referred to as IFT, consisted of the bidirectional movement of granule-like particles along the length of the flagella. These granule-like particles, averaging 0.5 ± 0.1 μm (n = 54, five cells) in diameter, could be seen as regions of high contrast (Fig. 1 *A* and *B*), but video-enhanced DIC microscopy was unable to resolve whether these regions of high contrast represented granules or waves moving in or beneath the plane of the flagellar membrane. In Fig. 1*B*, the movement of a prominent granule-like particle toward the flagellar tip (to the right) can be traced to the right of the diagonal white line. A difference-image sequence of the same flagellum, shown in Fig. 1*C*, indicates that each particle moved smoothly and continuously along the length of the flagellum with no change in direction or rate. Particles moving toward the flagellar base (to the left) were difficult to image in still frames; a greater number of particles than evident in Fig. 1*C* were seen in the real-time video images of this sequence. In Fig. 1*C*, the progress of individual particles toward the flagellar tip or base is bracketed by a diagonal line, the slope of which is the rate of movement.

The movement of the granule-like particles was quantified in M475, a paralyzed-flagella mutant of *C. moewusii* (15). In M475 cells, movement from the base to tip of the flagellum proceeded at 2.0 ± 0.5 μm/sec (n = 104, 12 cells); whereas, the movement from tip to base was similar in character but occurred at 3.5 ± 0.7 μm/sec (n = 50, 12 cells). To serve as an internal standard, the rates of two previously observed, nonbeat, flagellar motilities were also quantified. The gliding of cells by means of their flagella (Fig. 2*A*) across a glass coverslip occurred at 0.6 ± 0.2 μm/sec (n = 22), whereas the movement of polystyrene beads attached to the surface of the flagellar membrane (Fig. 2*B*) occurred at 1.1 ± 0.5 μm/sec (n = 20). Both values were similar to those reported (4, 5). Bead movement that occurs equally in both directions along the length of the flagellum in *C. reinhardtii* (5) was predominantly toward the flagellar base in *C. moewusii* M475 cells.

IFT was also observed in the flagella of both vegetative and gametic cells of *C. reinhardtii*, including mutants that lack the

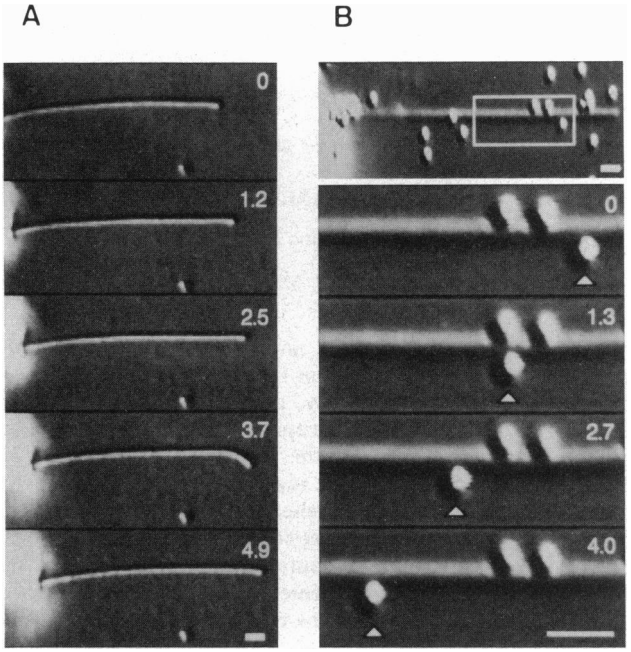

FIG. 2. Digital, video-enhanced DIC image sequences showing gliding and bead movement in *C. moewusii* M475 cells. All times are shown in seconds. (*A*) A single cell with its leading flagellum in contact with the substrate can be seen gliding across a glass coverslip, bringing the highly birefringent cell body into view. Stationary debris on the slide serves as a reference point. (*B*) A flagellum with several polystyrene beads (white spheres) attached to its surface. In the region of interest (white box), enlarged in the lower panels in a time-lapse manner, a single bead (0.31-μm diameter, arrowheads) was translocated toward the flagellar base; two other beads were attached but did not move. (Bar = 1 μm.)

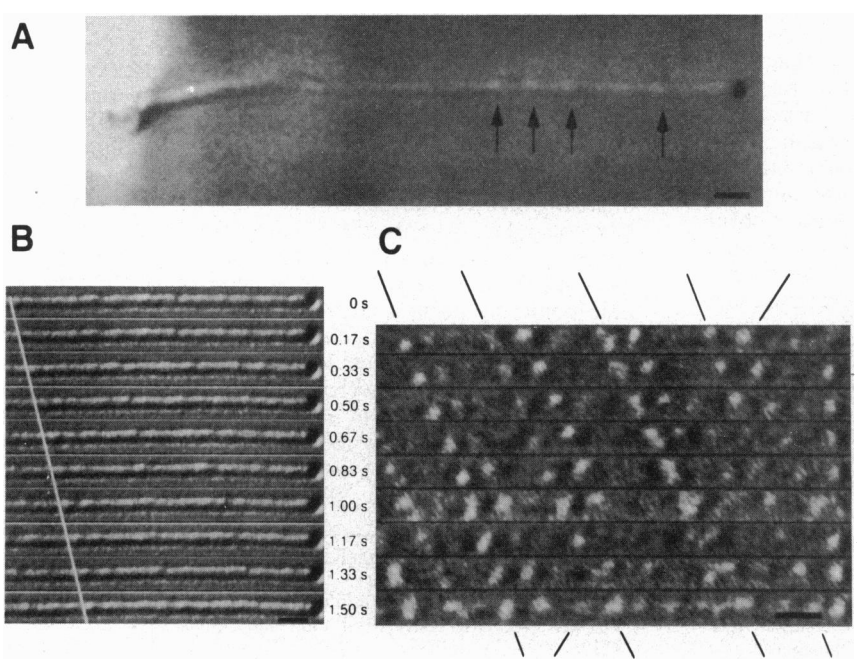

FIG. 1. Digital, video-enhanced DIC images illustrating IFT in *C. moewusii* (M475). (*A*) Granule-like particles are seen as high-contrast regions along the length of a flagellum (arrows); the birefringent cell body is located at left. (*B*) A time-lapse (seconds shown at right) enhanced-image sequence of a flagellum that shows movement of a granule-like particle (right of white line) toward the flagellar tip (to the right); other granule-like particles (not marked) can also be seen moving toward the flagellar tip. The sampling interval between each frame in this composite image and the one of *C* is 0.17 sec. (*C*) Difference-image sequence of the same flagellar region and time points shown in *B* that indicates the bidirectional movement of granule-like particles along the length of the flagellum. The vertical image height of each panel in the sequence equals the flagellar width. Only moving objects are visualized. (Bar = 1 μm.)

Table 1. Analysis of nonbeat flagellar motilities

Experiment	Bead movement	Gliding	IFT
Paralyzed *C. reinhardtii* mutant			
pf1 (radial spoke head deficient)	BD	+	+
pf18 vegetative cells (central pair deficient)	BD	+	+
pf18 gametes	BD	+	+
pf28 (outer dynein arm deficient)	BD	+	+
ida4 (inner dynein arm deficient)	BD	+	+
ida2 ida4 oda6 (outer and inner dynein arm deficient)	BD	+	+
Paralyzed *C. moewusii* mutant			
M475 (outer dynein arm deficient)	UD	+	+
gf1 (nongliding M475)	*	−	+
Flagellar regeneration and resorption			
M475, flagella regenerating (post pH shock)	UD	+	+
M475, flagella resorbing (low Ca^{2+}/25 mM sodium citrate)	−	−	+
pf18, flagella resorbing (0.5 mM IBMX)	BD	−/+	+
M475 cells			
EGTA [1 mM (<1 μM free Ca^{2+})]	−	−	+
$CdCl_2$ (25 μM)	BD	−/+	+
NaCl (100 mM)	−	−	−
Sucrose (6%)	−	−	−/+
Colchicine (2 mg/ml, 45 min)	UD	+	+
Cytochalasin D (200 μM, 45 min)	UD	+	+

+, Motility was observed; −, motility was not apparent; −/+, motility was observed, but it was reduced compared with wild-type or untreated cells; *, microsphere movement was observed but was negligible compared with M475; BD, bidirectional bead movement; UD, unidirectional bead movement toward the flagellar base; IBMX, 3-isobutyl-1-methylxanthine.

inner and/or outer dynein arms (16, 17) (Table 1). In addition, it was found that the *C. moewusii* paralyzed-flagella mutant M475 used for most of our IFT observations also lacks outer dynein arms (Fig. 3*A*). Therefore, IFT is not unique to a single species of *Chlamydomonas*, nor does it depend on the presence of flagellar dynein arms near the flagellar membrane.

IFT could be differentiated from polystyrene bead movement and gliding by the use of inhibitors and a nongliding mutant (Table 1). Most strikingly, low-free Ca^{2+} (<1 μM) reversibly inhibited both gliding and bead movement (18) but had no effect on IFT or adhesion of beads to the flagellar membrane. Similarly, IFT continued in the presence of Cd^{2+}, a Ca^{2+}-channel blocker (19, 20), which inhibited gliding and perturbed bead movement. IFT was also observed in a M475-derived mutant, gf1, that does not glide or properly translocate beads (21). Experimental separation of IFT from gliding and bead translocation suggested that IFT may be independent of these two motilities. In contrast, osmotically active molecules like NaCl and sucrose reversibly inhibited IFT along with gliding and bead translocation. The inhibition of IFT under conditions of increased osmotic pressure may be due to shrinkage of the flagellar membrane around the axoneme.

Because the flagellar axoneme assembles from the distal tip (22–25), flagellar precursors must move the length of the flagellum to reach the site of assembly. It was of interest, therefore, to observe IFT in cells induced to regenerate or resorb their flagella. Under these conditions, no change in the number or distribution of granule-like particles was apparent. Furthermore, the rates of IFT movement during flagellar regeneration and resorption resembled the rates seen in full-length flagella (Table 2).

The observations made with video-enhanced DIC microscopy suggested that IFT was occurring beneath the flagellar membrane; in support of this hypothesis, EM demonstrated the presence of complexes between the flagellar membrane and the outer doublet microtubules. These structures (arrowheads, Fig. 3 *A* and *D*) were observed in both *C. moewusii* (Fig. 3 *A* and *B*) and *C. reinhardtii* (Fig. 3 *C–F*), appearing ultrastructurally distinct from previously described bridges (small arrows, Fig. 3 *A* and *D*) between the axoneme and the flagellar/ciliary membrane of *Chlamydomonas* (26) or *Tetrahymena* (27–29). In longitudinal sections (Fig. 3 *B, C, E, F*), each complex appeared as a linear array of nonvesicular, lollipop-shaped structures distinct from the membrane (Fig. 3*F*). Within each array, the number of lollipop-shaped projections varied from a few to >40, appearing to attach the flagellar membrane to the axoneme. Although similar complexes have been seen on occasion (refs. 26 and 30; W. S. Sale, personal communication), we found in longitudinal and transverse sections that these complexes are not rare (Fig. 3 *A* and *C*). Several complexes were often observed in the same section and in sufficient number to account for the IFT observed with video-enhanced DIC microscopy (Fig. 3*C*). Examination of many different cross sections indicated that these complexes, which are clearly larger than the multicomponent dynein arms, were preferentially associated with the B tubules of the outer doublet microtubules.

DISCUSSION

The flagellum, like the neuronal axon, is a very long cell extension that requires the support of the cytoplasm for assembly, maintenance, and function. The motility described in this report, IFT, may be analogous to axonal transport, but unlike the axon, there are no membrane-bound vesicles being moved in the flagellum (26). Hence, IFT may represent the movement of non-vesicle-enclosed complexes, such as those shown in this report, along the length of the flagellum between the axoneme and the flagellar membrane. Except for the mitochondrion in the sperm midpiece, mitochondria and ribosomes are not present in the eukaryotic flagellum. Therefore, the nonvesicular complexes implicated in IFT may contain macromolecules (e.g., polypeptides, ATP), synthesized in the cell body, that are needed for flagellar assembly and/or function. To facilitate transport of these molecules to sites along the flagellum or to the distal tip where flagellar assembly occurs (22–25), one would expect the observed complexes to contain microtubule- or actin-based motors.

Epitopes recognized by antibodies against myosin-I, cytoplasmic dynein, kinesin, kinesin-related proteins, and actin

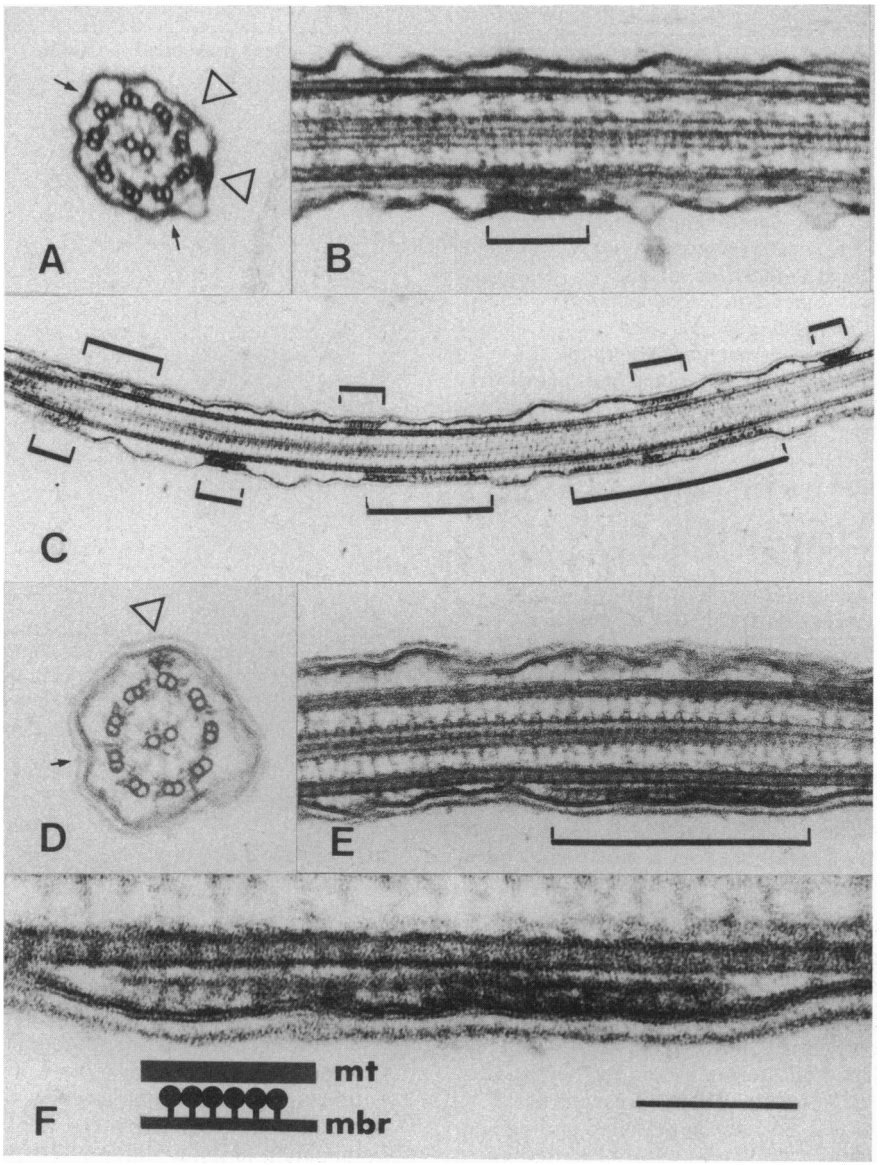

FIG. 3. Electron micrographs of complexes between the axonemal outer doublets and the flagellar membrane in both *C. moewusii* (*A* and *B*) and *C. reinhardtii* (*C–F*). In addition to these large complexes (arrowheads, *A* and *D*), small bridges are also shown (small arrows, *A* and *D*) between the flagellar membrane and the outer doublet microtubules. When viewed in longitudinal section (*B*, *C*, *E*, *F*), the large complexes appear as linear rafts of lollipop-shaped electron-dense projections. (*F*) Enlargement emphasizing the bracketed region of *E*. (mt, outer doublet microtubules; mbr, flagellar membrane.) (Bar in *F* = 0.23 μm for *A*, *B*, *D*, and *E*; 0.7 μm for *C*; and 0.1 μm for *F*.)

have been detected recently in preparations of whole flagella (31, 32). These motor epitopes remained with the axoneme after treatment of flagella with Nonidet P-40 (unpublished results), a treatment that does not release flagellar dynein (33). However, part of the epitope recognized by the antiactin antibody was released by detergent extraction. This result suggests that flagellar actin, previously shown to be associated with the inner dynein arms (34, 35), may also be positioned between the flagellar membrane and the outer doublet microtubules, perhaps as a submembranous microfilament network. This possibility is especially interesting, considering that epitopes recognized by myosin-I antibodies have been detected in the axonemal fractions of both *Chlamydomonas* flagella and several species of echinoderm sperm (M. Heintzelman and M. Mooseker, personal communication).

The epitopes recognized by antibodies against kinesin and kinesin-related proteins are also of particular interest. Recently, Fox *et al.* (32) have isolated a kinesin-related protein

Table 2. Rates of IFT in *C. moewusii* M475 cells

Flagellum	Mean rates of IFT, μm/sec	
	Toward flagellar tip	Toward flagellar base
Full length, untreated	2.0 ± 0.5 (n = 104, 12 cells)	3.5 ± 0.7 (n = 50, 12 cells)
Regenerating	1.9 ± 0.3 (n = 46, 9 cells)	3.3 ± 0.9 (n = 23, 7 cells)
Resorbing	2.0 ± 0.3 (n = 42, 5 cells)	3.5 ± 0.8 (n = 41, 11 cells)

Rates of IFT were measured as described (13). The mean rate and SD of IFT were calculated, where n is the number of granule-like particles measured. Conditions to induce flagellar resorption and regeneration are described in text.

from *Chlamydomonas* flagella and have demonstrated its binding *in vitro* to brain microtubules. Concomitantly, a *Chlamydomonas* gene encoding a member of the kinesin superfamily that appears flagella-specific has been cloned and sequenced (M. Bernstein, K.A.J., S. Katz, and J.L.R., unpublished work). A relationship between this kinesin isoform and IFT has not been established.

The difference in the rates of anterograde (to the flagellar tip) or retrograde (to the flagellar base) IFT suggests two different motor mechanisms. However, a single motor with bidirectional capability, as observed in *Reticulomyxa* (36, 37), cannot be ruled out. In the case of a single bidirectional motor, direction-dependent differences in the rates of IFT could result from either a change in the load placed on the motor, the switching of the motor between two different substrates, or a change in motor activity with respect to the direction of movement along a polarized substrate (e.g., microtubules).

To ascertain the mechanism and function of IFT, it will be necessary to identify the motors involved, the cargo carried by them, and whether the nonvesicular complexes observed with EM are, in fact, the granule-like particles observed moving in IFT. It also will be of interest to determine whether IFT is present in the cilia/flagella of other eukaryotes and in related structures, such as the connecting cilium of the rod photoreceptor cell. Regardless, *Chlamydomonas* exhibits a nonbeat, flagellar motility that will be very useful for studying the function of molecular motors because motor activity *in vivo* can be easily quantified by direct microscopic examination of the flagella.

We thank R. Kamiya for dynein mutants and U. Goodenough for EM protocols. We also thank R. Bloodgood, D. Diener, M. Heintzelman, M. Mooseker, and W. Sale for providing helpful comments on this manuscript or discussing unpublished results.

1. Bloodgood, R. A. (1990) in *Ciliary and Flagellar Membranes*, ed. Bloodgood, R. A. (Plenum, New York), pp. 91–128.
2. Bloodgood, R. A. (1992) *Biol. Cells* **76**, 291–302.
3. Lewin, R. A. (1952) *Biol. Bull. Woods Hole, Mass.* **103**, 74–79.
4. Bloodgood, R. A. (1981) *Protoplasma* **106**, 183–192.
5. Bloodgood, R. A. (1977) *J. Cell Biol.* **75**, 983–989.
6. Goodenough, U. W. & Jurivich, D. (1978) *J. Cell Biol.* **79**, 680–693.
7. Goodenough, U. W. (1991) in *Microbial Cell–Cell Interactions*, ed. Dworkin, M. (Am. Soc. Microbiol., Washington, DC), pp. 71–112.
8. Sager, R. & Granick, S. (1953) *Ann. N.Y. Acad. Sci.* **56**, 831–838.
9. Witman, G. B., Carlson, K., Berliner, J. & Rosenbaum, J. L. (1972) *J. Cell Biol.* **54**, 507–539.
10. Lefebvre, P. A., Nordstrom, S. A., Moulder, J. E. & Rosenbaum, J. L. (1978) *J. Cell Biol.* **78**, 8–27.
11. Lefebvre, P. A., Silflow, C. D., Wieben, E. D. & Rosenbaum, J. L. (1980) *Cell* **20**, 469–477.
12. Forscher, P. & Smith, S. J. (1988) *J. Cell Biol.* **107**, 1505–1516.
13. Forscher, P., Lin, C.-H. & Thompson, C. (1992) *Nature (London)* **357**, 515–518.
14. McDonald, K. (1984) *J. Ultrastruct. Res.* **86**, 107–118.
15. Lewin, R. A. (1952) *J. Gen. Microbiol.* **6**, 233–248.
16. Mitchell, D. R. & Rosenbaum, J. L. (1985) *J. Cell Biol.* **100**, 1228–1234.
17. Kamiya, R., Kurimoto, E. & Muto, E. (1991) *J. Cell Biol.* **112**, 441–447.
18. Bloodgood, R. A., Leffler, E. M. & Bojczuk, A. T. (1979) *J. Cell Biol.* **82**, 664–674.
19. Akaike, N., Lee, K. S. & Brown, A. M. (1978) *J. Gen. Physiol.* **71**, 509–531.
20. Fennikoh, K. B., Hirshfield, H. I. & Kneip, T. J. (1978) *Environ. Res.* **15**, 357–367.
21. Lewin, R. A. (1982) *Experientia* **38**, 348–349.
22. Rosenbaum, J. L. & Child, F. M. (1967) *J. Cell Biol.* **34**, 345–364.
23. Rosenbaum, J. L., Moulder, J. E. & Ringo, D. L. (1969) *J. Cell Biol.* **41**, 600–619.
24. Witman, G. B. (1975) *Ann. N.Y. Acad. Sci.* **253**, 178–191.
25. Johnson, K. A. & Rosenbaum, J. L. (1992) *J. Cell Biol.* **119**, 1605–1612.
26. Ringo, D. L. (1967) *J. Cell Biol.* **33**, 543–571.
27. Allen, R. D. (1968) *J. Cell Biol.* **37**, 825–831.
28. Sattler, C. A. & Staehelin, L. A. (1974) *J. Cell Biol.* **62**, 473–490.
29. Dentler, W. L., Pratt, M. M. & Stephens, R. E. (1980) *J. Cell Biol.* **84**, 381–403.
30. Mesland, D. A. M., Hoffman, J. L., Caligor, E. & Goodenough, U. W. (1980) *J. Cell Biol.* **84**, 599–617.
31. Kozminski, K. G., Johnson, K. A., Forscher, P. & Rosenbaum, J. L. (1992) *Mol. Biol. Cell* **3S**, 51 (abstr.).
32. Fox, L. A., Sawin, K. E. & Sale, W. S. (1992) *Mol. Biol. Cell* **3S**, 367 (abstr.).
33. Piperno, G. & Luck, D. J. L. (1979) *J. Biol. Chem.* **254**, 3084–3090.
34. Piperno, G. & Luck, D. J. L. (1979) *J. Biol. Chem.* **254**, 2187–2190.
35. Piperno, G., Mead, K. & Shestak, W. (1992) *J. Cell Biol.* **118**, 1455–1463.
36. Euteneuer, U., Koonce, M. P., Pfister, K. K. & Schliwa, M. (1988) *Nature (London)* **332**, 176–178.
37. Schliwa, M., Shimizu, T., Vale, R. D. & Euteneuer, U. (1991) *J. Cell Biol.* **112**, 1199–1203.